

Published in final edited form as:

Mol Pharm. 2013 April 1; 10(4): 1400–1408. doi:10.1021/mp3006984.

Design and Evaluation of New Tc-99m-Labeled Lactam Bridge-Cyclized Alpha-MSH Peptides for Melanoma Imaging

Haixun Guo[†], Fabio Gallazzi[§], and Yubin Miao^{†,‡,φ,*}

[†]College of Pharmacy, University of New Mexico, Albuquerque, NM 87131, USA

[‡]Cancer Research and Treatment Center, University of New Mexico, Albuquerque, NM 87131, USA

^φDepartment of Dermatology, University of New Mexico, Albuquerque, NM 87131, USA

[§]Department of Biochemistry, University of Missouri, Columbia, MO 65211, USA

Abstract

The purpose of this study was to examine the melanoma targeting and imaging properties of new ^{99m}Tc-labeled lactam bridge-cyclized alpha-melanocyte stimulating hormone (α-MSH) peptides using bifunctional chelating agents. MAG₃-GGNle-CycMSH_{hex}, AcCG₃-GGNle-CycMSH_{hex} and HYNIC-GGNle-CycMSH_{hex} peptides were synthesized and their melanocortin-1 (MC1) receptor binding affinities were determined in B16/F1 melanoma cells. The biodistribution of ^{99m}Tc-MAG₃-GGNle-CycMSH_{hex}, ^{99m}Tc-AcCG₃-GGNle-CycMSH_{hex}, ^{99m}Tc(CO)₃-HYNIC-GGNle-CycMSH_{hex} and ^{99m}Tc(EDDA)-HYNIC-GGNle-CycMSH_{hex} were determined in B16/F1 melanoma-bearing C57 mice at 2 h post-injection to select a lead peptide for further evaluation. The melanoma targeting and imaging properties of ^{99m}Tc(EDDA)-HYNIC-GGNle-CycMSH_{hex} were further examined because of its high melanoma uptake and fast urinary clearance. The IC₅₀ values of MAG₃-GGNle-CycMSH_{hex}, AcCG₃-GGNle-CycMSH_{hex} and HYNIC-GGNle-CycMSH_{hex} were 1.0 ± 0.05, 1.2 ± 0.19 and 0.6 ± 0.04 nM in B16/F1 melanoma cells, respectively. Among these four ^{99m}Tc-peptides, ^{99m}Tc(EDDA)-HYNIC-GGNle-CycMSH_{hex} exhibited the highest melanoma uptake (14.14 ± 4.90% ID/g) and fastest urinary clearance (91.26 ± 1.96% ID) at 2 h post-injection. ^{99m}Tc(EDDA)-HYNIC-GGNle-CycMSH_{hex} showed high tumor to normal organ uptake ratios except for the kidneys. The tumor/kidney uptake ratios of ^{99m}Tc(EDDA)-HYNIC-GGNle-CycMSH_{hex} were 2.50 and 3.55 at 4 and 24 h post-injection. The melanoma lesions were clearly visualized by SPECT/CT using ^{99m}Tc(EDDA)-HYNIC-GGNle-CycMSH_{hex} as an imaging probe at 2 h post-injection. Overall, high melanoma uptake coupled with fast urinary clearance of ^{99m}Tc(EDDA)-HYNIC-GGNle-CycMSH_{hex} highlighted its potential for metastatic melanoma detection in the future.

Keywords

Alpha-melanocyte stimulating hormone; ^{99m}Tc-labeled lactam bridge-cyclized peptide; melanoma SPECT imaging

INTRODUCTION

Skin cancer is the most commonly diagnosed cancer in the United States. Approximately 3.5 millions skin cancers are diagnosed annually. Among the three major types of skin cancer

(basal cell carcinoma, squamous cell carcinoma and melanoma), melanoma is the most deadly skin cancer with an increasing incidence rate.¹ Although melanoma only accounts for less than 5% of skin cancer cases, it results in greater than 75% of deaths from skin cancer. The cancer statistics from American Cancer Society predicted that 9,180 deaths of melanoma would occur in the United States in 2012.¹ Unfortunately, no curative treatment is available for metastatic melanoma. Early diagnosis followed by a prompt surgical removal offers patients the best opportunities for cures or prolonged survivals. Thus, it has been of great interest to develop receptor-targeting peptide radiopharmaceuticals for melanoma imaging and therapy.^{2–19}

We and others have reported radiolabeled lactam bridge-cyclized α -MSH peptides targeting melanocortin-1 (MC1) receptors for melanoma imaging over the past a few years.^{20–29} We have developed two generations of α -MSH peptides cyclized either via a Lys-Asp or an Asp-Lys lactam bridge. The first-generation peptides were built on the backbone of CycMSH peptide {c[Lys-Nle-Glu-His-DPhe-Arg-Trp-Gly-Arg-Pro-Val-Asp]}, whereas the second-generation peptides were designed based upon the construct of CycMSH_{hex} peptide {c[Asp-His-DPhe-Arg-Trp-Lys]-CONH₂}. DOTA (1,4,7,10-tetraazacyclododecane-1,4,7,10-tetraacetic acid) was attached to the CycMSH and CycMSH_{hex} peptides for ¹¹¹In labeling. Compared to the first-generation ¹¹¹In-labeled CycMSH peptides, the second-generation ¹¹¹In-labeled CycMSH_{hex} peptides exhibited enhanced melanoma uptake and decreased renal uptake.^{20–25} Among the ¹¹¹In-labeled CycMSH_{hex} peptides, we identified ¹¹¹In-DOTA-GGNle-CycMSH_{hex} as a lead peptide because of its high melanoma uptake (19.05 ± 5.04 % ID/g at 2 h post-injection) and relatively low renal uptake (6.84 ± 0.92 % ID/g at 2 h post-injection) in B16/F1 melanoma-bearing C57 mice.²⁵ The melanoma lesions could be clearly visualized by single photon emission computed tomography (SPECT) using ¹¹¹In-DOTA-GGNle-CycMSH_{hex} as an imaging probe.²⁵

Despite the success of ¹¹¹In-DOTA-GGNle-CycMSH_{hex} for melanoma imaging, we managed to develop new ^{99m}Tc-labeled CycMSH_{hex} peptides for melanoma imaging due to the wide utilization of ^{99m}Tc as a diagnostic radionuclide in nuclear medicine. Technetium-99m is an ideal SPECT radionuclide because of its 140-keV γ -photon emission and a manageable 6 h half-life. Meanwhile, ^{99m}Tc is very cost-effective and can be easily obtained from a commercial ⁹⁹Mo-^{99m}Tc generator. High melanoma uptake of ¹¹¹In-DOTA-GGNle-CycMSH_{hex} underscored it as a lead peptide construct. Thus, we managed to develop new ^{99m}Tc-labeled GGNle-CycMSH_{hex} peptides using different ^{99m}Tc chelators for melanoma imaging in this study. Mercaptoacetyltriglycine (MAG₃) and Ac-Cys-Gly-Gly-Gly (AcCG₃) are N₃S chelators for ^{99m}Tc, whereas hydrazinonicotinamide (HYNIC) can form ^{99m}Tc complexes via either an IsoLink™ carbonyl labeling agent or Ethylenediaminediacetic acid (EDDA)/Tricine solution. Therefore, we replaced the DOTA chelator with three different bifunctional chelating agents, namely MAG₃, AcCG₃ and HYNIC, to generate new MAG₃-GGNle-CycMSH_{hex}, AcCG₃-GGNle-CycMSH_{hex} and HYNIC-GGNle-CycMSH_{hex} peptides to examine which chelating agent was the best in retaining favorable melanoma targeting and pharmacokinetic properties. We determined their MC1 receptor binding affinities in B16/F1 melanoma cells first. Then, we examined the biodistribution of ^{99m}Tc-MAG₃-GGNle-CycMSH_{hex}, ^{99m}Tc-AcCG₃-GGNle-CycMSH_{hex}, ^{99m}Tc(CO)₃-HYNIC-GGNle-CycMSH_{hex} and ^{99m}Tc(EDDA)-HYNIC-GGNle-CycMSH_{hex} at 2 h post-injection to select a lead ^{99m}Tc-peptide for further evaluation. ^{99m}Tc(EDDA)-HYNIC-GGNle-CycMSH_{hex} displayed the highest melanoma uptake and fastest urinary clearance. Therefore, we further determined the biodistribution of ^{99m}Tc(EDDA)-HYNIC-GGNle-CycMSH_{hex} and its property for molecular imaging in B16/F1 melanoma-bearing C57 mice in this study.

EXPERIMENTAL SECTION

Chemicals and Reagents

Amino acids and resin were purchased from Advanced ChemTech Inc. (Louisville, KY) and Novabiochem (San Diego, CA). Boc-HYNIC was purchased from VWR International, Inc. (Albuquerque, NM). ^{125}I -Tyr²-[Nle⁴, D-Phe⁷]- α -MSH { ^{125}I -(Tyr²)-NDP-MSH} was obtained from PerkinElmer, Inc. (Waltham, MA) for receptor binding assays. $^{99\text{m}}\text{TcO}_4^-$ was purchased from Cardinal Health (Albuquerque, NM) for peptide radiolabeling. All other chemicals used in this study were purchased from Thermo Fischer Scientific (Waltham, MA) and used without further purification. B16/F1 murine melanoma cells were obtained from American Type Culture Collection (Manassas, VA).

Peptide Synthesis and Receptor Binding Assay

MAG₃-GGNle-CycMSH_{hex}, AcCG₃-GGNle-CycMSH_{hex} and HYNIC-GGNle-CycMSH_{hex} were synthesized using fluorenylmethyloxy carbonyl (Fmoc) chemistry, purified by reverse phase-high performance liquid chromatography (RP-HPLC) and characterized by liquid chromatography-mass spectrometry (LC-MS). Generally, 70 μmol of resin, 210 μmol of each Fmoc-protected amino acid and 210 μmol of Boc-HYNIC were used for the synthesis. Briefly, the intermediate scaffolds of Mercaptoacetyl(Trt)-Gly-Gly-Gly-Gly-Gly-Nle-Asp(O-2-PhiPr)-His(Trt)-DPhe-Arg(Pbf)-Trp(Boc)-Lys(Dde), A c-Cys-Gly-Gly-Gly-Gly-Gly-Nle-Asp(O-2-PhiPr)-His(Trt)-DPhe-Arg(Pbf)-Trp(Boc)-Lys(Dde) and HYNIC(Boc)-Gly-Gly-Nle-Asp(O-2-PhiPr)-His(Trt)-DPhe-Arg(Pbf)-Trp(Boc)-Lys(Dde) were synthesized on H₂N-Sieber amide resin using an Advanced ChemTech multiple-peptide synthesizer (Louisville, KY). The protecting group of Dde was removed by 2% hydrazine for peptide cyclization. The protecting group of 2-phenylisopropyl was removed and the protected peptide was cleaved from the resin by treating with a mixture of 2.5% of trifluoroacetic acid (TFA) and 5% of triisopropylsilane. Each protected peptide was cyclized by coupling the carboxylic group from the Asp with the epsilon amino group from the Lys. The cyclization reaction was achieved by an overnight reaction in N,N-dimethylformamide (DMF) using benzotriazole-1-yl-oxy-tris-pyrrolidino-phosphonium-hexafluorophosphate (PyBOP) as a coupling agent in the presence of N,N-diisopropylethylamine (DIPEA). Each protected cyclic peptide was dissolved in H₂O/CH₃CN (50:50) and lyophilized to remove the reagents. The protecting groups were totally removed by treating with a mixture of TFA, thioanisole, phenol, water, ethanedithiol and triisopropylsilane (87.5:2.5:2.5:2.5:2.5:2.5) for 2 h at room temperature (25 °C). Each peptide was precipitated and washed with ice-cold ether four times, purified by RP-HPLC and characterized by LC-MS. The MC1 receptor binding affinities (IC₅₀ values) of MAG₃-GGNle-CycMSH_{hex}, AcCG₃-GGNle-CycMSH_{hex} and HYNIC-GGNle-CycMSH_{hex} were determined in B16/F1 melanoma cells by *in vitro* competitive receptor binding assays according to our published procedure.²⁵ The study was carried out in triplicate, the final IC₅₀ value was calculated by averaging two experiments.

Peptide Radiolabeling with $^{99\text{m}}\text{Tc}$

$^{99\text{m}}\text{Tc}$ -MAG₃-GGNle-CycMSH_{hex} and $^{99\text{m}}\text{Tc}$ -AcCG₃-GGNle-CycMSH_{hex} were prepared according to the published procedure³⁰ with modifications. Briefly, 10 μL of 1 mg/mL MAG₃-GGNle-CycMSH_{hex} or AcCG₃-GGNle-CycMSH_{hex} aqueous solution, 10 μL of pH 9.2 tartrate buffer (50 $\mu\text{g}/\mu\text{L}$ Na₂tartrate·2H₂O, 0.5 M Na₂HCO₃, 0.25 M NH₄OAc, 0.175 M NH₃), 3 μL of freshly prepared tin chloride solution (10 $\mu\text{g}/\mu\text{L}$ SnCl₂·2H₂O, 1 $\mu\text{g}/\mu\text{L}$ sodium ascorbate, 10 mM HCl), and 50 μL of $^{99\text{m}}\text{TcO}_4^-$ solution (37–74 MBq) were added into a reaction vial and incubated at 100 °C for 20 min. Each radiolabeled peptide was purified to a single species by Waters RP-HPLC (Milford, MA) on a Grace Vydac C-18 reverse phase analytical column (Deerfield, IL) using a 20-min gradient of 22–32% acetonitrile in 20 mM HCl aqueous solution at a flow rate of 1 mL/min. The mobile phase

consisted of solvent A (20 mM HCl aqueous solution) and solvent B (100% CH₃CN). The gradient was initiated and kept at 78:22 A/B for 3 min followed by a linear gradient of 78:22 A/B to 68:32 A/B over 20 min. Then, the gradient was changed from 68:32 A/B to 10:90 A/B over 3 min followed by an additional 5 min at 10:90 A/B. Thereafter, the gradient was changed from 10:90 A/B to 78:22 A/B over 3 min. Each purified peptide was purged with N₂ gas for 20 min to remove the acetonitrile. The pH of the final solution was adjusted to 5 with 0.1 N NaOH and normal saline for animal studies.

^{99m}Tc(CO)₃-HYNIC-GGNle-CycMSH_{hex} was prepared using an IsoLink™ carbonyl labeling agent (DRN4335; Mallinckrodt). First, 1 mL of ^{99m}TcO₄⁻ (185 MBq) solution was added into an IsoLink™ kit and incubated at 100°C for 20 min to yield [^{99m}Tc(CO)₃(OH)₂]₃⁺. Second, 200 μL of the [^{99m}Tc(CO)₃(OH)₂]₃⁺ preparation and 10 μL of 1 mg/mL HYNIC-GGNle-CycMSH_{hex} aqueous solution were added into 200 μL of 0.5 M NH₄OAc buffer (pH 5.44) in a reaction vial and incubated at 75°C for 30 min. The radiolabeled peptide was purified to a single species by Waters RP-HPLC on a Grace Vydac C-18 reverse phase analytical column using a 20-min gradient of 24–34% acetonitrile in 20 mM HCl aqueous solution at a flow rate of 1 mL/min. The purified peptide was purged with N₂ gas for 20 min to remove the acetonitrile. The pH of the final solution was adjusted to 5 with 0.1 N NaOH and normal saline for animal studies.

^{99m}Tc(EDDA)-HYNIC-GGNle-CycMSH_{hex} was prepared according to the published procedure³¹ with modifications. Briefly, 50 μL of ^{99m}TcO₄⁻ (37–74 MBq), 10 μL of 1 mg/mL SnCl₂ in 0.1 N HCl solution, 200 μL of a mixture of 5 mg/mL of EDDA and 25 mg/mL of Tricine aqueous solution and 10 μL of 1 mg/mL HYNIC-GGNle-CycMSH_{hex} aqueous solution were added into 400 μL of 0.5 M NH₄OAc (pH 5.44) in a reaction vial and incubated at 95°C for 30 min. The radiolabeled peptide was purified to a single species using a Waters RP-HPLC on a Grace Vydac C-18 reverse phase analytical column using a 20-min gradient of 18–28% acetonitrile in 20 mM HCl aqueous solution at a flow rate of 1 mL/min. The purified peptide was purged with N₂ gas for 20 min to remove the acetonitrile. The pH of the final solution was adjusted to 5 with 0.1 N NaOH and normal saline for animal studies.

Biodistribution Studies

All animal studies were conducted in compliance with Institutional Animal Care and Use Committee approval. In an attempt to select a lead ^{99m}Tc-peptide for further evaluation, the biodistribution of ^{99m}Tc-MAG₃-GGNle-CycMSH_{hex}, ^{99m}Tc-AcCG₃-GGNle-CycMSH_{hex}, ^{99m}Tc(CO)₃-HYNIC-GGNle-CycMSH_{hex} and ^{99m}Tc(EDDA)-HYNIC-GGNle-CycMSH_{hex} were examined in B16/F1 melanoma-bearing C57 female mice (Harlan, Indianapolis, IN) at 2 h post-injection, respectively. The C57 mice were subcutaneously inoculated with 1×10⁶ B16/F1 cells on the right flank for each mouse to generate B16/F1 tumors. The weights of tumors reached approximately 0.2 g 10 days post cell inoculation. Each melanoma-bearing mouse was injected with 0.037 MBq of ^{99m}Tc-MAG₃-GGNle-CycMSH_{hex}, ^{99m}Tc-AcCG₃-GGNle-CycMSH_{hex}, ^{99m}Tc(CO)₃-HYNIC-GGNle-CycMSH_{hex} or ^{99m}Tc(EDDA)-HYNIC-GGNle-CycMSH_{hex} via the tail vein. Groups of 5 mice were sacrificed at 2 h post-injection, tumor and organs of interest were harvested, weighed and counted in a Wallace 1480 automated gamma counter (PerkinElmer). Meanwhile, intestines and urine were collected and counted to evaluate the clearance pathway of each ^{99m}Tc-labeled peptide. Blood was taken as 6.5% of the body weight.

^{99m}Tc(EDDA)-HYNIC-GGNle-CycMSH_{hex} displayed higher melanoma uptake and faster urinary clearance than the other three ^{99m}Tc-peptides. Therefore, its biodistribution properties were further determined in B16/F1 melanoma-bearing C57 female mice at 0.5, 4 and 24 h post-injection. The B16/F1 melanoma-bearing mice were generated as described

above. Each melanoma-bearing mouse was injected with 0.037 MBq of $^{99m}\text{Tc}(\text{EDDA})\text{-HYNIC-GGNle-CycMSH}_{\text{hex}}$ via the tail vein. Groups of 5 mice were sacrificed at 0.5, 4 and 24 h post-injection, and tumors and organs of interest were harvested, weighed and counted. Blood was taken as 6.5% of the body weight. The tumor uptake specificity of $^{99m}\text{Tc}(\text{EDDA})\text{-HYNIC-GGNle-CycMSH}_{\text{hex}}$ was determined by co-injecting 10 μg (6.07 nmol) of unlabeled NDP-MSH peptide at 2 h post-injection. To examine whether L-lysine co-injection could decrease the renal uptake, a group of 5 mice was injected with a mixture of 12 mg of L-lysine and 0.037 MBq of $^{99m}\text{Tc}(\text{EDDA})\text{-HYNIC-GGNle-CycMSH}_{\text{hex}}$. The mice were sacrificed at 2 h post-injection and the tumors and organs of interest were harvested, weighed and counted.

Melanoma Imaging and Urinary Metabolites of $^{99m}\text{Tc}(\text{EDDA})\text{-HYNIC-GGNle-CycMSH}_{\text{hex}}$

Approximately 7.4 MBq of $^{99m}\text{Tc}(\text{EDDA})\text{-HYNIC-GGNle-CycMSH}_{\text{hex}}$ was injected into a B16/F1 melanoma-bearing C57 mouse for melanoma imaging and urine metabolites analysis. The mouse was euthanized at 2 h post-injection for small animal SPECT/CT (Nano-SPECT/CT[®], Bioscan) imaging, as well as to collect urine for analyzing the metabolites. The 9-min CT imaging was immediately followed by the whole-body SPECT scan. The SPECT scans of 24 projections were acquired. Reconstructed SPECT and CT data were visualized and co-registered using InVivoScope (Bioscan, Washington DC). The collected urine sample was centrifuged at 16,000 *g* for 5 min before the HPLC analysis. Thereafter, aliquots of the urine were injected into the HPLC. A 20-minute gradient of 18–28% acetonitrile/20 mM HCl with a flow rate of 1 mL/min was used for urine analysis.

Statistical Analysis

Statistical analysis was performed using the Student's t-test for unpaired data. A 95% confidence level was chosen to determine the significance of difference in tumor and renal uptake of $^{99m}\text{Tc}(\text{EDDA})\text{-HYNIC-GGNle-CycMSH}_{\text{hex}}$ with/without NDP-MSH co-injection, as well as the significance of difference in tumor and renal uptake of $^{99m}\text{Tc}(\text{EDDA})\text{-HYNIC-GGNle-CycMSH}_{\text{hex}}$ with/without L-lysine co-injection in the biodistribution studies described above. The differences at the 95% confidence level ($p < 0.05$) were considered significant.

RESULTS

New $\text{MAG}_3\text{-GGNle-CycMSH}_{\text{hex}}$, $\text{AcCG}_3\text{-GGNle-CycMSH}_{\text{hex}}$ and $\text{HYNIC-GGNle-CycMSH}_{\text{hex}}$ were synthesized and purified by RP-HPLC. The overall synthetic yields were 25–30% for $\text{MAG}_3\text{-GGNle-CycMSH}_{\text{hex}}$, $\text{AcCG}_3\text{-GGNle-CycMSH}_{\text{hex}}$ and $\text{HYNIC-GGNle-CycMSH}_{\text{hex}}$. All three peptides displayed greater than 90% purity after HPLC purification. The identities of $\text{MAG}_3\text{-GGNle-CycMSH}_{\text{hex}}$, $\text{AcCG}_3\text{-GGNle-CycMSH}_{\text{hex}}$ and $\text{HYNIC-GGNle-CycMSH}_{\text{hex}}$ were confirmed by electrospray ionization mass spectrometry. The calculated and measured molecular weights of $\text{MAG}_3\text{-GGNle-CycMSH}_{\text{hex}}$, $\text{AcCG}_3\text{-GGNle-CycMSH}_{\text{hex}}$ and $\text{HYNIC-GGNle-CycMSH}_{\text{hex}}$ are presented in Table 1. The measured molecular weights matched the calculated molecular weights. The schematic structures of $\text{MAG}_3\text{-GGNle-CycMSH}_{\text{hex}}$, $\text{AcCG}_3\text{-GGNle-CycMSH}_{\text{hex}}$ and $\text{HYNIC-GGNle-CycMSH}_{\text{hex}}$ are shown in Figure 1. The IC_{50} values of $\text{MAG}_3\text{-GGNle-CycMSH}_{\text{hex}}$, $\text{AcCG}_3\text{-GGNle-CycMSH}_{\text{hex}}$ and $\text{HYNIC-GGNle-CycMSH}_{\text{hex}}$ were 1.0 ± 0.05 , 1.2 ± 0.19 and 0.6 ± 0.04 nM in B16/F1 melanoma cells, respectively (Table 1).

Both $\text{MAG}_3\text{-GGNle-CycMSH}_{\text{hex}}$ and $\text{AcCG}_3\text{-GGNle-CycMSH}_{\text{hex}}$ were readily labeled with ^{99m}Tc with greater than 95% radiolabeling yields in tartrate buffer using SnCl_2 as a reducing agent. $^{99m}\text{Tc-MAG}_3\text{-GGNle-CycMSH}_{\text{hex}}$ and $^{99m}\text{Tc-AcCG}_3\text{-GGNle-CycMSH}_{\text{hex}}$ were completely separated from their excess non-labeled peptides by RP-HPLC. The

retention times of ^{99m}Tc -MAG₃-GGNle-CycMSH_{hex} and ^{99m}Tc -AcCG₃-GGNle-CycMSH_{hex} were 14.9 and 13.0 min, whereas the retention times of MAG₃-GGNle-CycMSH_{hex} and AcCG₃-GGNle-CycMSH_{hex} were 12.0 and 12.0 min, respectively. Both ^{99m}Tc -MAG₃-GGNle-CycMSH_{hex} and ^{99m}Tc -AcCG₃-GGNle-CycMSH_{hex} showed greater than 98% radiochemical purities after HPLC purification. HYNIC-GGNle-CycMSH_{hex} was radiolabeled with ^{99m}Tc either via an IsoLink™ carbonyl labeling agent or EDDA/Tricine solution with greater than 95% radiolabeling yields. $^{99m}\text{Tc}(\text{CO})_3$ -HYNIC-GGNle-CycMSH_{hex} and $^{99m}\text{Tc}(\text{EDDA})$ -HYNIC-GGNle-CycMSH_{hex} were completely separated from their excess non-labeled peptides by RP-HPLC. The retention times of $^{99m}\text{Tc}(\text{CO})_3$ -HYNIC-GGNle-CycMSH_{hex} and $^{99m}\text{Tc}(\text{EDDA})$ -HYNIC-GGNle-CycMSH_{hex} were 18.0 and 17.9 min, whereas the retention time of HYNIC-GGNle-CycMSH_{hex} was 15.5 min. Both $^{99m}\text{Tc}(\text{CO})_3$ -HYNIC-GGNle-CycMSH_{hex} and $^{99m}\text{Tc}(\text{EDDA})$ -HYNIC-GGNle-CycMSH_{hex} displayed greater than 98% radiochemical purities after HPLC purification.

The melanoma targeting and pharmacokinetic properties of ^{99m}Tc -MAG₃-GGNle-CycMSH_{hex}, ^{99m}Tc -AcCG₃-GGNle-CycMSH_{hex}, $^{99m}\text{Tc}(\text{CO})_3$ -HYNIC-GGNle-CycMSH_{hex} and $^{99m}\text{Tc}(\text{EDDA})$ -HYNIC-GGNle-CycMSH_{hex} were determined in B16/F1 melanoma-bearing mice at 2 h post-injection to select a lead radiolabeled peptide for further evaluation. The biodistribution results of these four ^{99m}Tc -conjugates are shown in Table 2. Although ^{99m}Tc -MAG₃-GGNle-CycMSH_{hex} and $^{99m}\text{Tc}(\text{CO})_3$ -HYNIC-GGNle-CycMSH_{hex} displayed substantial tumor uptake of $4.64 \pm 1.06\%$ ID/g and $5.84 \pm 1.26\%$ ID/g at 2 h post-injection, $^{99m}\text{Tc}(\text{CO})_3$ -HYNIC-GGNle-CycMSH_{hex} showed higher liver uptake (38.11 ± 2.31 vs. $1.18 \pm 0.15\%$ ID/g) and renal uptake (17.69 ± 4.06 vs. $1.20 \pm 0.51\%$ ID/g) than ^{99m}Tc -MAG₃-GGNle-CycMSH_{hex} at 2 h post-injection. Meanwhile, ^{99m}Tc -AcCG₃-GGNle-CycMSH_{hex} displayed improved melanoma uptake of $9.76 \pm 0.51\%$ ID/g coupled with low liver and renal uptake (1.69 ± 0.35 and $2.62 \pm 0.45\%$ ID/g, respectively) at 2 h post-injection. $^{99m}\text{Tc}(\text{EDDA})$ -HYNIC-GGNle-CycMSH_{hex} exhibited the highest tumor uptake ($14.14 \pm 4.90\%$ ID/g) among these four ^{99m}Tc -conjugates at 2 h post-injection in B16/F1 melanoma-bearing C57 mice. Interestingly, $^{99m}\text{Tc}(\text{CO})_3$ -HYNIC-GGNle-CycMSH_{hex} showed the highest renal and liver uptake, as well as the highest accumulation in blood, heart, lung, spleen, stomach, bone and skin at 2 h post-injection among these four ^{99m}Tc -conjugates. Compared to $^{99m}\text{Tc}(\text{CO})_3$ -HYNIC-GGNle-CycMSH_{hex}, both ^{99m}Tc -MAG₃-GGNle-CycMSH_{hex} and ^{99m}Tc -AcCG₃-GGNle-CycMSH_{hex} displayed much lower normal organ accumulation at 2 h post-injection. The uptake of ^{99m}Tc -MAG₃-GGNle-CycMSH_{hex} or ^{99m}Tc -AcCG₃-GGNle-CycMSH_{hex} was lower than 3.4% ID/g in stomach, liver and kidneys at 2 h post-injection. However, only 27.53 ± 6.99% ID of ^{99m}Tc -MAG₃-GGNle-CycMSH_{hex} and 38.20 ± 3.98% ID of ^{99m}Tc -AcCG₃-GGNle-CycMSH_{hex} were excreted through the urinary system, while 55.02 ± 10.44% ID of ^{99m}Tc -MAG₃-GGNle-CycMSH_{hex} and 50.91 ± 2.72% ID of ^{99m}Tc -AcCG₃-GGNle-CycMSH_{hex} were excreted through the GI system. On the other hand, $^{99m}\text{Tc}(\text{EDDA})$ -HYNIC-GGNle-CycMSH_{hex} exhibited the highest tumor uptake ($14.14 \pm 4.90\%$ ID/g) and the fastest urinary clearance ($91.26 \pm 1.96\%$ ID) at 2 h post-injection. Thus, we selected $^{99m}\text{Tc}(\text{EDDA})$ -HYNIC-GGNle-CycMSH_{hex} as a lead peptide to further examine its full biodistribution and melanoma imaging properties.

The full biodistribution results of $^{99m}\text{Tc}(\text{EDDA})$ -HYNIC-GGNle-CycMSH_{hex} are presented in Table 3. $^{99m}\text{Tc}(\text{EDDA})$ -HYNIC-GGNle-CycMSH_{hex} displayed high tumor uptake and prolonged tumor retention in B16/F1 melanoma-bearing C57 mice. The tumor uptake was $13.75 \pm 3.49\%$ ID/g at 30 min post-injection and reached its peak value of $14.14 \pm 4.90\%$ ID/g at 2 h post-injection. Compared with the tumor uptake at 2 h post-injection, 93.6% of the radioactivity remained in the tumor at 4 h post-injection. In the melanoma uptake blocking study, co-injection of NDP-MSH blocked 96.8% of the tumor uptake ($p < 0.05$) at 2

h post-injection, demonstrating that the tumor uptake was MC1 receptor-mediated. Normal organ uptake of $^{99m}\text{Tc}(\text{EDDA})\text{-HYNIC-GGNle-CycMSH}_{\text{hex}}$ was lower than 1.02% ID/g in normal tissues except for kidneys at 2, 4 and 24 h post-injection. High tumor/blood and high tumor/normal organ uptake ratios were achieved as early as 0.5 h post-injection. As the major excretion pathway of $^{99m}\text{Tc}(\text{EDDA})\text{-HYNIC-GGNle-CycMSH}_{\text{hex}}$, the kidney uptake was $11.21 \pm 1.68\%$ ID/g at 0.5 h post-injection and decreased to $1.28 \pm 0.28\%$ ID/g at 24 h post-injection. The tumor/kidney uptake ratios of $^{99m}\text{Tc}(\text{EDDA})\text{-HYNIC-GGNle-CycMSH}_{\text{hex}}$ were 1.88, 2.50 and 3.55 at 2, 4 and 24 h post-injection. Co-injection of NDP-MSH didn't reduce the renal uptake of the $^{99m}\text{Tc}(\text{EDDA})\text{-HYNIC-GGNle-CycMSH}_{\text{hex}}$ activity at 2 h post-injection, indicating that the renal uptake was not MC1 receptor-mediated. Meanwhile, *L*-lysine co-injection decreased 42% of the renal uptake ($p < 0.05$) without affecting the tumor uptake. Moreover, $^{99m}\text{Tc}(\text{EDDA})\text{-HYNIC-GGNle-CycMSH}_{\text{hex}}$ exhibited rapid urinary excretion. Approximately 91% of the activity cleared out of the body at 2 h post-injection. The representative whole-body, coronal and transversal SPECT/CT images are presented in Figure 2. The melanoma lesions were clearly visualized by SPECT/CT using $^{99m}\text{Tc}(\text{EDDA})\text{-HYNIC-GGNle-CycMSH}_{\text{hex}}$ as an imaging probe at 2 h post-injection. $^{99m}\text{Tc}(\text{EDDA})\text{-HYNIC-GGNle-CycMSH}_{\text{hex}}$ exhibited high tumor to normal organ uptake ratios except for the kidneys, which was consistent with the biodistribution results. Urinary metabolites of $^{99m}\text{Tc}(\text{EDDA})\text{-HYNIC-GGNle-CycMSH}_{\text{hex}}$ were analyzed by RP-HPLC 2 h post-injection. The radioactive HPLC profile of urine is illustrated in Figure 3. The urine analysis suggested that $^{99m}\text{Tc}(\text{EDDA})\text{-HYNIC-GGNle-CycMSH}_{\text{hex}}$ remained intact in urine at 2 h post-injection.

DISCUSSION

It has been of interest to develop ^{99m}Tc -labeled α -MSH peptides targeting the MC1 receptors for melanoma imaging. Both linear and cyclic ^{99m}Tc -labeled α -MSH peptides were reported for melanoma targeting. Specifically, bifunctional chelator Ac-Cys-Gly-Cys-Gly- (for ^{99m}Tc radiolabeling) was coupled to the N-terminus of the linear NDP-MSH peptide to generate $^{99m}\text{Tc}\text{-CGCG-NDPMSH}$.³² $^{99m}\text{Tc}\text{-CGCG-NDPMSH}$ displayed $6.52 \pm 1.11\%$ ID/g of tumor uptake in B16/F1 melanoma-bearing C57 mice at 30 min post-injection. However, $^{99m}\text{Tc}\text{-CGCG-NDPMSH}$ showed a rapid tumor washout. The tumor uptake of $^{99m}\text{Tc}\text{-CGCG-NDPMSH}$ dramatically decreased to $0.56 \pm 0.14\%$ ID/g at 4 h post-injection. Meanwhile, $^{99m}\text{Tc}\text{-CGCG-NDPMSH}$ exhibited high liver uptake (6.80 ± 1.22 and $4.58 \pm 1.02\%$ ID/g) at 30 min and 1 h post-injection. Another bifunctional chelator MAG_2 (tetrafluorophenyl mercaptoacetylglucylglycyl-gamma-aminobutyrate) was coupled to the epsilon amino group of Lys¹¹ to yield $^{99m}\text{Tc}\text{-MAG}_2\text{-NDPMSH}$. Compared to $^{99m}\text{Tc}\text{-CGCG-NDPMSH}$, $^{99m}\text{Tc}\text{-MAG}_2\text{-NDPMSH}$ showed lower tumor uptake (4.17 ± 1.34 and $2.39 \pm 1.21\%$ ID/g at 30 min and 1 h post-injection) in B16/F1 melanoma-bearing C57 mice.³²

It was an interesting approach to introduce three cysteines at the 3rd, 4th and 10th position of CCMSH peptide for preparing $^{99m}\text{Tc}\text{-CCMSH}$. Three Cys^{3,4,10} sulfhydryls and one Cys⁴ amide nitrogen in the CCMSH peptide provided a site-specific chelator for complexing ^{99m}Tc .^{2,3,33} Importantly, $^{99m}\text{Tc}\text{-CCMSH}$ exhibited dramatically enhanced tumor uptake and prolonged tumor retention compared to $^{99m}\text{Tc}\text{-CGCG-NDPMSH}$ in B16/F1 melanoma-bearing C57 mice. The tumor uptake of $^{99m}\text{Tc}\text{-CCMSH}$ was 12.97 ± 1.38 and $11.64 \pm 1.54\%$ ID/g at 30 min and 1 h post-injection, respectively. The tumor uptake of $^{99m}\text{Tc}\text{-CCMSH}$ was $9.51 \pm 1.97\%$ ID/g at 4 h post-injection, which was 16.98 times the tumor uptake of $^{99m}\text{Tc}\text{-CGCG-NDPMSH}$ at 4 h post-injection.^{3,32} Furthermore, the substitution of Lys¹¹ with Arg¹¹ generated $^{99m}\text{Tc}\text{-(Arg}^{11}\text{)CCMSH}$, which exhibited enhanced tumor uptake and dramatically reduced renal uptake in B16/F1 melanoma-bearing C57 mice.¹⁸ The tumor uptake of $^{99m}\text{Tc}\text{-(Arg}^{11}\text{)CCMSH}$ was 1.21 and 1.17 times the tumor

uptake of ^{99m}Tc -CCMSH at 1 and 4 h post-injection, whereas the renal uptake of ^{99m}Tc -(Arg¹¹)CCMSH was only 59.2% and 37.9% of the renal uptake of ^{99m}Tc -CCMSH at 1 and 4 h post-injection.^{3,18} High tumor uptake and reduced renal uptake highlighted ^{99m}Tc -(Arg¹¹)CCMSH as a lead metal-cyclized imaging probe for melanoma detection.

A lactam bridge-cyclized α -MSH peptide was radiolabeled with the $^{99m}\text{Tc}(\text{CO})_3$ core to generate $^{99m}\text{Tc}(\text{CO})_3$ -pz- β Ala-Nle-cyclo[Asp-His-DPhe-Arg-Trp-Lys]-NH₂.²⁶ Not surprisingly, $^{99m}\text{Tc}(\text{CO})_3$ -pz- β Ala-Nle-cyclo[Asp-His-DPhe-Arg-Trp-Lys]-NH₂ exhibited high tumor uptake and prolonged tumor retention. The tumor uptake of $^{99m}\text{Tc}(\text{CO})_3$ -pz- β Ala-Nle-cyclo[Asp-His-DPhe-Arg-Trp-Lys]-NH₂ was 9.26 ± 0.83 and $11.31 \pm 1.83\%$ ID/g at 1 h and 4 h post-injection, respectively. Unfortunately, $^{99m}\text{Tc}(\text{CO})_3$ -pz- β Ala-Nle-cyclo[Asp-His-DPhe-Arg-Trp-Lys]-NH₂ showed extremely high renal and liver uptake at 1 and 4 h post-injection. The renal uptake of $^{99m}\text{Tc}(\text{CO})_3$ -pz- β Ala-Nle-cyclo[Asp-His-DPhe-Arg-Trp-Lys]-NH₂ was $71.06 \pm 6.44\%$ and $32.12 \pm 1.57\%$ ID/g at 1 and 4 h post-injection, whereas the liver uptake of $^{99m}\text{Tc}(\text{CO})_3$ -pz- β Ala-Nle-cyclo[Asp-His-DPhe-Arg-Trp-Lys]-NH₂ was 42.19 ± 5.05 and $22.86 \pm 1.17\%$ ID/g at 1 and 4 h post-injection.²⁶

In this study, we developed new ^{99m}Tc -labeled lactam bridge-cyclized α -MSH peptides building upon the GGNle-CycMSH_{hex} peptide construct we identified.²⁵ Specifically, we coupled three bifunctional chelating agents, namely MAG₃, AcCG₃ and HYNIC, to GGNle-CycMSH_{hex} to generate new MAG₃-GGNle-CycMSH_{hex}, AcCG₃-GGNle-CycMSH_{hex} and HYNIC-GGNle-CycMSH_{hex} peptides. The coupling of MAG₃, AcCG₃ and HYNIC to GGNle-CycMSH_{hex} retained low nanomolar MC1 receptor binding affinities of the peptides. The IC₅₀ was 1.0 ± 0.05 nM for MAG₃-GGNle-CycMSH_{hex}, 1.2 ± 0.19 nM for AcCG₃-GGNle-CycMSH_{hex} and 0.6 ± 0.04 nM HYNIC-GGNle-CycMSH_{hex} (Table 1), respectively. It is worthwhile to note that both MAG₃ and AcCG₃ provide N₃S chelators for ^{99m}Tc conjugation, whereas the HYNIC chelator allows ^{99m}Tc conjugation via either the $^{99m}\text{Tc}(\text{CO})_3$ or $^{99m}\text{Tc}(\text{EDDA})$ core. Therefore, we prepared ^{99m}Tc -MAG₃-GGNle-CycMSH_{hex}, ^{99m}Tc -AcCG₃-GGNle-CycMSH_{hex}, $^{99m}\text{Tc}(\text{CO})_3$ -HYNIC-GGNle-CycMSH_{hex} and $^{99m}\text{Tc}(\text{EDDA})$ -HYNIC-GGNle-CycMSH_{hex} conjugates in this study. Furthermore, we determined their biodistribution properties in B16/F1 melanoma-bearing C57 mice at 2 h post-injection to examine which bifunctional chelator was the best in retaining favorable melanoma targeting and pharmacokinetic properties. Despite the slight difference in receptor binding affinity among MAG₃-GGNle-CycMSH_{hex}, AcCG₃-GGNle-CycMSH_{hex} and HYNIC-GGNle-CycMSH_{hex}, we observed dramatic differences in melanoma uptake, accumulation in non-target tissues, and excretion pathways among these four ^{99m}Tc -conjugates. As shown in Table 2, ^{99m}Tc -MAG₃-GGNle-CycMSH_{hex} and $^{99m}\text{Tc}(\text{CO})_3$ -HYNIC-GGNle-CycMSH_{hex} showed substantial tumor uptake, whereas ^{99m}Tc -AcCG₃-GGNle-CycMSH_{hex} displayed enhanced melanoma uptake. $^{99m}\text{Tc}(\text{EDDA})$ -HYNIC-GGNle-CycMSH_{hex} exhibited the highest tumor uptake among these four ^{99m}Tc -peptides at 2 h post-injection in B16/F1 melanoma-bearing C57 mice. It was worthwhile to note that $^{99m}\text{Tc}(\text{CO})_3$ -HYNIC-GGNle-CycMSH_{hex} exhibited high liver and renal uptake, as well as higher accumulation in the normal organs than the other three ^{99m}Tc -peptides at 2 h post-injection. It was likely that ^{99m}Tc was demetallated from the peptide *in vivo*. Obviously, the disadvantage associated with ^{99m}Tc -MAG₃-GGNle-CycMSH_{hex} and ^{99m}Tc -AcCG₃-GGNle-CycMSH_{hex} was the accumulation in the GI system. Approximately $55.02 \pm 10.44\%$ ID of ^{99m}Tc -MAG₃-GGNle-CycMSH_{hex} and $50.91 \pm 2.72\%$ ID of ^{99m}Tc -AcCG₃-GGNle-CycMSH_{hex} were excreted through the GI system. On the other hand, $^{99m}\text{Tc}(\text{EDDA})$ -HYNIC-GGNle-CycMSH_{hex} exhibited the fastest urinary clearance ($91.26 \pm 1.96\%$ ID) at 2 h post-injection. Thus, we further examined the full biodistribution and melanoma imaging properties of $^{99m}\text{Tc}(\text{EDDA})$ -HYNIC-GGNle-CycMSH_{hex}.

As shown in Table 3, $^{99m}\text{Tc}(\text{EDDA})\text{-HYNIC-GGNle-CycMSH}_{\text{hex}}$ displayed high tumor uptake and prolonged tumor retention in B16/F1 melanoma-bearing C57 mice. The tumor uptake reached its peak value of $14.14 \pm 4.90\%$ ID/g at 2 h post-injection, with 93.6% of the radioactivity remaining in tumor at 4 h post-injection. Co-injection of NDP-MSH blocked 96.8% of tumor uptake ($p < 0.05$) without affecting the renal uptake at 2 h post-injection, demonstrating that the tumor uptake was MC1 receptor-mediated and the renal uptake was non-specific. Meanwhile, *L*-lysine co-injection decreased 42% of the renal uptake ($p < 0.05$) without affecting the tumor uptake, indicating that the overall positive charge of the ^{99m}Tc -peptide contributed to the non-specific renal uptake. It was worthwhile to note that there was a positively-charged side chain in Arg⁸, which is critical for MC1 receptor binding. $^{99m}\text{Tc}(\text{EDDA})\text{-HYNIC-GGNle-CycMSH}_{\text{hex}}$ exhibited low accumulation in normal organs and a rapid urinary excretion, resulting in high tumor to normal organ uptake ratios. As we anticipated, the B16/F1 melanoma lesions were clearly visualized by SPECT/CT using $^{99m}\text{Tc}(\text{EDDA})\text{-HYNIC-GGNle-CycMSH}_{\text{hex}}$ as an imaging probe.

At the present time, $^{99m}\text{Tc}(\text{Arg}^{11})\text{CCMSH}$ displayed more favorable melanoma targeting and pharmacokinetic properties than $^{99m}\text{Tc}(\text{CO})_3\text{-pz-}\beta\text{Ala-Nle-cyclo[Asp-His-DPhe-Arg-Trp-Lys]-NH}_2$ and $^{99m}\text{Tc-CGCG-NDPMSH}$. Although $^{99m}\text{Tc}(\text{CO})_3\text{-pz-}\beta\text{Ala-Nle-cyclo[Asp-His-DPhe-Arg-Trp-Lys]-NH}_2$ showed similar high tumor uptake ($11.31 \pm 1.81\%$ ID/g) with $^{99m}\text{Tc}(\text{Arg}^{11})\text{CCMSH}$, $^{99m}\text{Tc}(\text{CO})_3\text{-pz-}\beta\text{Ala-Nle-cyclo[Asp-His-DPhe-Arg-Trp-Lys]-NH}_2$ displayed high accumulation and prolonged retention in both liver ($22.86 \pm 1.17\%$ ID/g) and kidneys ($32.12 \pm 1.57\%$ ID/g) at 4 h post-injection. High liver and renal uptake of $^{99m}\text{Tc}(\text{CO})_3\text{-pz-}\beta\text{Ala-Nle-cyclo[Asp-His-DPhe-Arg-Trp-Lys]-NH}_2$ would limit its potential application in metastatic melanoma imaging. Remarkably, $^{99m}\text{Tc}(\text{EDDA})\text{-HYNIC-GGNle-CycMSH}_{\text{hex}}$ exhibited comparably high melanoma uptake ($13.23 \pm 2.35\%$ ID/g) to $^{99m}\text{Tc}(\text{Arg}^{11})\text{CCMSH}$ at 4 h post-injection. Importantly, as shown in Figure 4, $^{99m}\text{Tc}(\text{EDDA})\text{-HYNIC-GGNle-CycMSH}_{\text{hex}}$ displayed faster urinary clearance than $^{99m}\text{Tc}(\text{Arg}^{11})\text{CCMSH}$ (92.3% ID vs. 83.8% ID) and much lower intestinal accumulation than $^{99m}\text{Tc}(\text{Arg}^{11})\text{CCMSH}$ (1.9% ID vs. 11.5% ID) at 4 h post-injection. The differences in intestinal accumulation and urinary clearance were likely due to the structural differences between $^{99m}\text{Tc}(\text{EDDA})\text{-HYNIC-GGNle-CycMSH}_{\text{hex}}$ and $^{99m}\text{Tc}(\text{Arg}^{11})\text{CCMSH}$.

In conclusion, the biodistribution of $^{99m}\text{Tc-MAG}_3\text{-GGNle-CycMSH}_{\text{hex}}$, $^{99m}\text{Tc-AcCG}_3\text{-GGNle-CycMSH}_{\text{hex}}$, $^{99m}\text{Tc}(\text{CO})_3\text{-HYNIC-GGNle-CycMSH}_{\text{hex}}$ and $^{99m}\text{Tc}(\text{EDDA})\text{-HYNIC-GGNle-CycMSH}_{\text{hex}}$ were determined in B16/F1 melanoma-bearing C57 mice in this study. Among these four ^{99m}Tc -peptides, $^{99m}\text{Tc}(\text{EDDA})\text{-HYNIC-GGNle-CycMSH}_{\text{hex}}$ exhibited the highest melanoma uptake and fastest urinary clearance at 2 h post-injection. Overall, the properties of high melanoma uptake, low accumulation in intestines and fast urinary clearance of $^{99m}\text{Tc}(\text{EDDA})\text{-HYNIC-GGNle-CycMSH}_{\text{hex}}$ highlighted its potential as an imaging probe for metastatic melanoma detection in the future.

Acknowledgments

We thank Dr. Jianquan Yang for their technical assistance. This work was supported in part by the NIH grant NM-INBRE P20RR016480/P20GM103451 and University of New Mexico HSC RAC Award. The image in this article was generated by the Keck-UNM Small Animal Imaging Resource established with funding from the W.M. Keck Foundation and the University of New Mexico Cancer Research and Treatment Center (NIH P30 CA118100).

References

1. Jemal A, Siegel R, Xu J, Ward E. Cancer statistics. *CA Cancer J Clin.* 2010; 60:277–300. [PubMed: 20610543]

2. Giblin MF, Wang NN, Hoffman TJ, Jurisson SS, Quinn TP. Design and characterization of α -melanotropin peptide analogs cyclized through rhenium and technetium metal coordination. *Proc Natl Acad Sci US A*. 1998; 95:12814–12818.
3. Chen J, Cheng Z, Hoffman TJ, Jurisson SS, Quinn TP. Melanoma-targeting properties of ^{99m}Tc -labeled cyclic alpha-melanocyte-stimulating hormone peptide analogues. *Cancer Res*. 2000; 60:5649–5658. [PubMed: 11059756]
4. Chen J, Cheng Z, Owen NK, Hoffman TJ, Miao Y, Jurisson SS, Quinn TP. Evaluation of an ^{111}In -DOTA-rhenium cyclized alpha-MSH analog: a novel cyclic-peptide analog with improved tumor-targeting properties. *J Nucl Med*. 2001; 42:1847–1855. [PubMed: 11752084]
5. Miao Y, Owen NK, Whitener D, Gallazzi F, Hoffman TJ, Quinn TP. In vivo evaluation of ^{188}Re -labeled alpha-melanocyte stimulating hormone peptide analogs for melanoma therapy. *Int J Cancer*. 2002; 101:480–487. [PubMed: 12216078]
6. Froidevaux S, Calame-Christe M, Tanner H, Sumanovski L, Eberle AN. A novel DOTA-alpha-melanocyte-stimulating hormone analog for metastatic melanoma diagnosis. *J Nucl Med*. 2002; 43:1699–1706. [PubMed: 12468522]
7. Cheng Z, Chen J, Miao Y, Owen NK, Quinn TP, Jurisson SS. Modification of the structure of a metalloprotein: synthesis and biological evaluation of ^{111}In -labeled DOTA-conjugated rhenium-cyclized alpha-MSH analogues. *J Med Chem*. 2002; 45:3048–3056. [PubMed: 12086490]
8. Miao Y, Whitener D, Feng W, Owen NK, Chen J, Quinn TP. Evaluation of the human melanoma targeting properties of radiolabeled alpha-melanocyte stimulating hormone peptide analogues. *Bioconjug Chem*. 2003; 14:1177–1184. [PubMed: 14624632]
9. Froidevaux S, Calame-Christe M, Schuhmacher J, Tanner H, Saffrich R, Henze M, Eberle AN. A gallium-labeled DOTA-alpha-melanocyte-stimulating hormone analog for PET imaging of melanoma metastases. *J Nucl Med*. 2004; 45:116–123. [PubMed: 14734683]
10. Miao Y, Owen NK, Fisher DR, Hoffman TJ, Quinn TP. Therapeutic efficacy of a ^{188}Re -labeled alpha-melanocyte-stimulating hormone peptide analog in murine and human melanoma-bearing mouse models. *J Nucl Med*. 2005; 46:121–129. [PubMed: 15632042]
11. Froidevaux S, Calame-Christe M, Tanner H, Eberle AN. Melanoma targeting with DOTA-alpha-melanocyte-stimulating hormone analogs: structural parameters affecting tumor uptake and kidney uptake. *J Nucl Med*. 2005; 46:887–895. [PubMed: 15872364]
12. Miao Y, Hylarides M, Fisher DR, Shelton T, Moore H, Wester DW, Fritzbeg AR, Winkelmann CT, Hoffman TJ, Quinn TP. Melanoma therapy via peptide-targeted alpha-radiation. *Clin Cancer Res*. 2005; 11:5616–5621. [PubMed: 16061880]
13. McQuade P, Miao Y, Yoo J, Quinn TP, Welch MJ, Lewis JS. Imaging of melanoma using ^{64}Cu - and ^{86}Y -DOTA-ReCCMSH(Arg11), a cyclized peptide analogue of alpha-MSH. *J Med Chem*. 2005; 48:2985–2992. [PubMed: 15828837]
14. Miao Y, Hoffman TJ, Quinn TP. Tumor-targeting properties of ^{90}Y - and ^{177}Lu -labeled α -melanocyte stimulating hormone peptide analogues in a murine melanoma model. *Nucl Med Biol*. 2005; 32:485–493. [PubMed: 15982579]
15. Miao Y, Fisher DR, Quinn TP. Reducing renal uptake of ^{90}Y and ^{177}Lu labeled alpha-melanocyte stimulating hormone peptide analogues. *Nucl Med Biol*. 2006; 33:723–733. [PubMed: 16934691]
16. Wei L, Butcher C, Miao Y, Gallazzi F, Quinn TP, Welch MJ, Lewis JS. Synthesis and biologic evaluation of ^{64}Cu -labeled rhenium-cyclized alpha-MSH peptide analog using a cross-bridged cyclam chelator. *J Nucl Med*. 2007; 48:64–72. [PubMed: 17204700]
17. Cheng Z, Xiong Z, Subbarayan M, Chen X, Gambhir SS. ^{64}Cu -labeled alpha-melanocyte-stimulating hormone analog for MicroPET imaging of melanocortin 1 receptor expression. *Bioconjug Chem*. 2007; 18:765–772. [PubMed: 17348700]
18. Miao Y, Benwell K, Quinn TP. ^{99m}Tc - and ^{111}In -labeled alpha-melanocyte-stimulating hormone peptides as imaging probes for primary and pulmonary metastatic melanoma detection. *J Nucl Med*. 2007; 48:73–80. [PubMed: 17204701]
19. Miao Y, Shelton T, Quinn TP. Therapeutic efficacy of a ^{177}Lu -labeled DOTA conjugated alpha-melanocyte-stimulating hormone peptide in a murine melanoma-bearing mouse model. *Cancer Biother Radiopharm*. 2007; 22:333–341. [PubMed: 17651039]

20. Miao Y, Gallazzi F, Guo H, Quinn TP. ^{111}In -labeled lactam bridge-cyclized alpha-melanocyte stimulating hormone peptide analogues for melanoma imaging. *Bioconjug Chem.* 2008; 19:539–547. [PubMed: 18197608]
21. Guo H, Shenoy N, Gershman BM, Yang J, Sklar LA, Miao Y. Metastatic melanoma imaging with an ^{111}In -labeled lactam bridge-cyclized alpha-melanocyte-stimulating hormone peptide. *Nucl Med Biol.* 2009; 36:267–276. [PubMed: 19324272]
22. Guo H, Yang J, Gallazzi F, Prossnitz ER, Sklar LA, Miao Y. Effect of DOTA position on melanoma targeting and pharmacokinetic properties of ^{111}In -labeled lactam bridge-cyclized α -melanocyte stimulating hormone peptide. *Bioconjug Chem.* 2009; 20:2162–2168. [PubMed: 19817405]
23. Guo H, Yang J, Shenoy N, Miao Y. Gallium-67-labeled lactam bridge-cyclized alpha-melanocyte stimulating hormone peptide for primary and metastatic melanoma imaging. *Bioconjug Chem.* 2009; 20:2356–2363. [PubMed: 19919057]
24. Guo H, Yang J, Gallazzi F, Miao Y. Reduction of the ring size of radiolabeled lactam bridge-cyclized alpha-MSH peptide resulting in enhanced melanoma uptake. *J Nucl Med.* 2010; 51:418–426. [PubMed: 20150256]
25. Guo H, Yang J, Gallazzi F, Miao Y. Effects of the amino acid linkers on melanoma-targeting and pharmacokinetic properties of Indium-111-labeled lactam bridge-cyclized α -MSH peptides. *J Nucl Med.* 2011; 52:608–616. [PubMed: 21421725]
26. Raposinho PD, Xavier C, Correia JD, Falcao S, Gomes P, Santos I. Melanoma targeting with alpha-melanocyte stimulating hormone analogs labeled with fac- $^{99\text{m}}\text{Tc}(\text{CO})_3]^+$: effect of cyclization on tumor-seeking properties. *J Biol Inorg Chem.* 2008; 13:449–459. [PubMed: 18183429]
27. Raposinho PD, Correia JD, Alves S, Botelho MF, Santos AC, Santos I. A $^{99\text{m}}\text{Tc}(\text{CO})_3$ -labeled pyrazolyl- α -melanocyte-stimulating hormone analog conjugate for melanoma targeting. *Nucl Med Biol.* 2008; 35:91–99. [PubMed: 18158948]
28. Guo H, Miao Y. Cu-64-labeled lactam bridge-cyclized alpha-MSH peptides for PET imaging of melanoma. *Mol Pharmaceutics.* 2012; 9:2322–2330.
29. Guo H, Gallazzi F, Miao Y. Ga-67-labeled lactam bridge-cyclized alpha-MSH peptides with enhanced melanoma uptake and reduced renal uptake. *Bioconjug Chem.* 2012; 23:1341–1348.
30. Liu G, Dou S, He J, Yin D, Gupta S, Zhang S, Wang Y, Rusckowski M, Hnatowich DJ. Radiolabeling of MAG_3 -morpholino oligomers with ^{188}Re at high labeling efficiency and specific radioactivity for tumor pretargeting. *Appl Radiat Isot.* 2006; 64:971–978. [PubMed: 16730997]
31. Liu S, Edwards S, Looby RJ, Harris AR, Poirier MJ, Barrett JA, Heminway SJ, Carroll TR. Labeling a hydrazino nictinamide-modified cyclic IIb/IIIa receptor antagonist with $^{99\text{m}}\text{Tc}$ using aminocarboxylates as coligands. *Bioconjug Chem.* 1996; 7:63–71. [PubMed: 8741992]
32. Chen J, Giblin MF, Wang N, Jurisson SS, Quinn TP. In vivo evaluation of $^{99\text{m}}\text{Tc}/^{188}\text{Re}$ -labeled linear alpha-melanocyte stimulating hormone analogs for specific melanoma targeting. *Nucl Med Biol.* 1999; 26:687–693. [PubMed: 10587108]
33. Giblin MF, Jurisson SS, Quinn TP. Synthesis and characterization of rhenium-complexed α -melanotropin analogs. *Bioconjug Chem.* 1997; 8:347–353. [PubMed: 9177840]

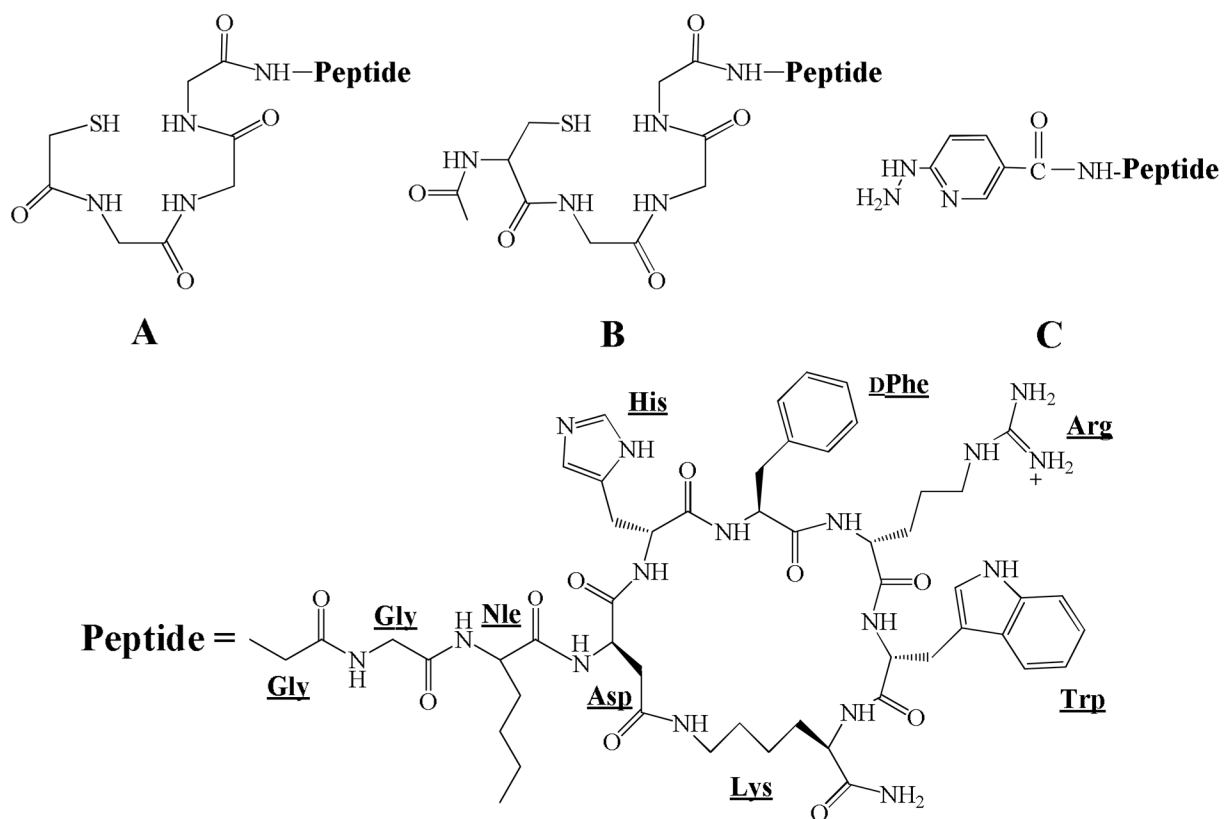


Figure 1.
Schematic structures of MAG₃-GGNle-CycMSH_{hex} (A), AcCG₃-GGNle-CycMSH_{hex} (B)
and HYNIC-GGNle-CycMSH_{hex} (C).

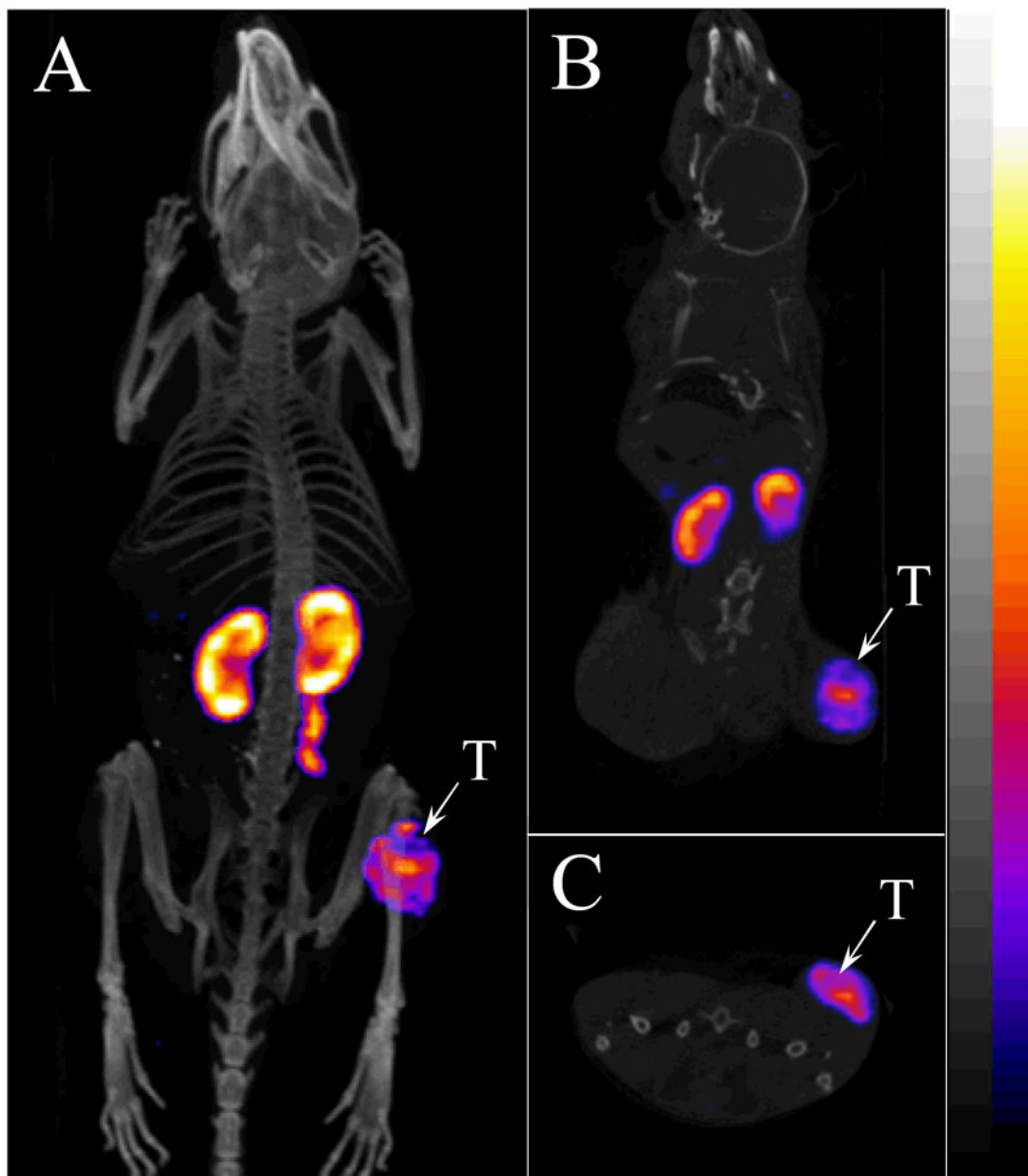


Figure 2. Representative whole-body (A), coronal (B) and transversal (C) SPECT/CT images of $^{99m}\text{Tc}(\text{EDDA})\text{-HYNIC-GGNle-CycMSH}_{\text{hex}}$ in a B16/F1 melanoma-bearing C57 mouse at 2 h post-injection. The tumor lesions (T) were highlighted with arrows on the images.

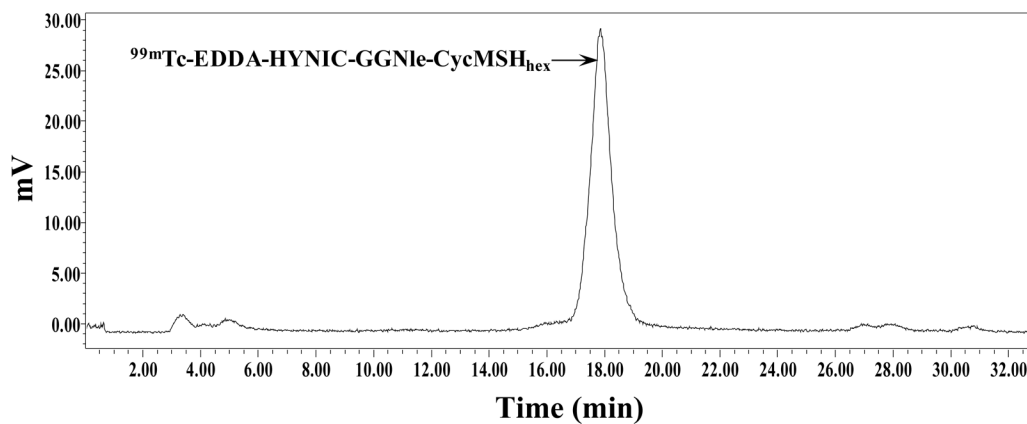


Figure 3. Radioactive HPLC profile of urine sample of a B16/F1 melanoma-bearing C57 mouse at 2 h post-injection of $^{99m}\text{Tc(EDDA)-HYNIC-GGNle-CycMSH}_{\text{hex}}$. The arrow indicates the retention time (17.9 min) of the original compound of $^{99m}\text{Tc(EDDA)-HYNIC-GGNle-CycMSH}_{\text{hex}}$ prior to the tail vein injection.

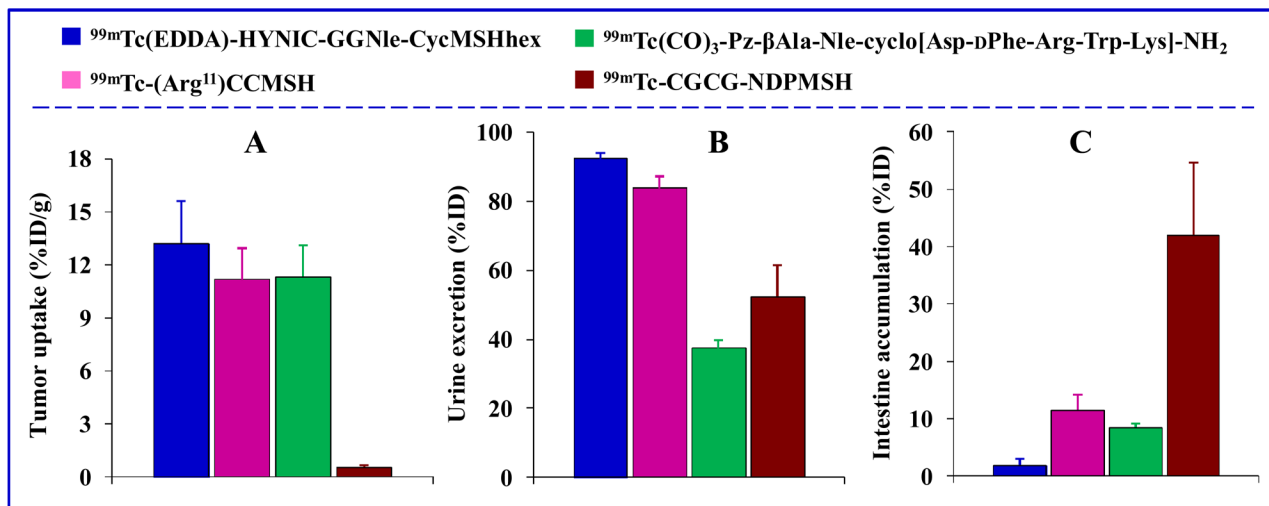


Figure 4. Comparisons in tumor uptake (A), urine excretion (B) and intestine accumulation (C) at 4 h post-injection among $^{99m}\text{Tc}(\text{EDDA})\text{-HYNIC-GGNle-CycMSH}_{\text{hex}}$ (blue), $^{99m}\text{Tc}(\text{Arg}^{11})\text{CCMSH}$ (pink), $^{99m}\text{Tc}(\text{CO})_3\text{-Pz-}\beta\text{Ala-Nle-cyclo[Asp-His-DPhe-Arg-Trp-Lys]NH}_2$ (green) and $^{99m}\text{Tc-CGCG-NDPMSH}$ (red). Data of $^{99m}\text{Tc}(\text{Arg}^{11})\text{CCMSH}$, $^{99m}\text{Tc}(\text{CO})_3\text{-Pz-}\beta\text{Ala-Nle-cyclo[Asp-His-DPhe-Arg-Trp-Lys]NH}_2$ and $^{99m}\text{Tc-CGCG-NDPMSH}$ were cited from references 18, 26 and 32 for comparison.

Table 1

IC₅₀ values and molecular weights (MWs) of MAG₃-GGNle-CycMSH_{hex}, AcCG₃-GGNle-CycMSH_{hex} and HYNIC-GGNle-CycMSH_{hex}.

Peptide	IC ₅₀ (nM)	Calculated MW	Measured MW
MAG ₃ -GGNle-CycMSH _{hex}	1.0 ± 0.05	1340.6	1341.0
AcCG ₃ -GGNle-CycMSH _{hex}	1.2 ± 0.19	1411.6	1412.1
HYNIC-GGNle-CycMSH _{hex}	0.6 ± 0.04	1231.0	1230.8

Table 2

Biodistribution comparison among ^{99m}Tc -MAG₃-GGNle-CycMSH_{hex} {MAG₃}, ^{99m}Tc -AcCG₃-GGNle-CycMSH_{hex} {AcCG₃}, ^{99m}Tc (CO)₃-HYNIC-GGNle-CycMSH_{hex} {(CO)₃} and ^{99m}Tc (EDDA)-HYNIC-GGNle-CycMSH_{hex} {EDDA} in B16/F1 melanoma-bearing C57 mice at 2 h post-injection. The data were presented as percent injected dose/gram or as percent injected dose (Mean \pm SD, n=5)

Tissues	MAG ₃	AcCG ₃	(CO) ₃	EDDA
Percent injected dose/gram (%ID/g)				
Tumor	4.64 \pm 1.06	9.76 \pm 0.51	5.84 \pm 1.26	14.14 \pm 4.90
Brain	0.05 \pm 0.05	0.04 \pm 0.03	0.12 \pm 0.02	0.05 \pm 0.04
Blood	0.25 \pm 0.13	0.27 \pm 0.13	2.17 \pm 1.91	0.17 \pm 0.05
Heart	0.33 \pm 0.13	0.27 \pm 0.14	1.94 \pm 0.22	0.09 \pm 0.03
Lung	0.46 \pm 0.10	0.47 \pm 0.09	4.42 \pm 1.62	0.41 \pm 0.06
Liver	1.18 \pm 0.15	1.69 \pm 0.35	38.11 \pm 2.31	0.52 \pm 0.05
Spleen	0.30 \pm 0.12	0.35 \pm 0.10	4.70 \pm 1.13	0.18 \pm 0.08
Stomach	3.38 \pm 0.78	2.86 \pm 1.80	4.01 \pm 1.78	1.02 \pm 0.31
Kidneys	1.20 \pm 0.51	2.62 \pm 0.45	17.69 \pm 4.06	7.52 \pm 0.96
Muscle	0.08 \pm 0.02	0.12 \pm 0.09	0.17 \pm 0.07	0.04 \pm 0.02
Pancreas	0.41 \pm 0.54	0.32 \pm 0.16	1.02 \pm 0.55	0.04 \pm 0.04
Bone	0.29 \pm 0.13	0.50 \pm 0.28	1.91 \pm 0.52	0.12 \pm 0.05
Skin	0.28 \pm 0.10	0.20 \pm 0.07	1.75 \pm 0.62	0.33 \pm 0.10
Percent injected dose (%ID)				
Intestines	55.02 \pm 10.44	50.91 \pm 2.72	18.35 \pm 5.49	1.09 \pm 0.06
Urine	27.53 \pm 6.99	38.20 \pm 3.98	27.65 \pm 2.53	91.26 \pm 1.96

Biodistribution of $^{99m}\text{Tc}(\text{EDDA})\text{-HYNIC-GGNIe-CycMSH}_{\text{hex}}$ in B16/F1 melanoma-bearing C57 mice. The data were presented as percent injected dose/gram or as percent injected dose (Mean \pm SD, n=5)

Table 3

Tissues	0.5 h	2 h [#]	4 h	24 h	2-h NDP blockade	2-h L-Lys co-injection
	Percent injected dose/gram (%ID/g)					
Tumor	13.75 \pm 3.49	14.14 \pm 4.90	13.23 \pm 2.35	4.54 \pm 0.70	0.45 \pm 0.29*	14.10 \pm 2.90
Brain	0.10 \pm 0.02	0.05 \pm 0.04	0.03 \pm 0.04	0.01 \pm 0.01	0.01 \pm 0.01	0.03 \pm 0.02
Blood	2.62 \pm 0.09	0.17 \pm 0.05	0.12 \pm 0.08	0.03 \pm 0.01	0.24 \pm 0.07	0.09 \pm 0.05
Heart	0.84 \pm 0.31	0.09 \pm 0.03	0.05 \pm 0.04	0.02 \pm 0.02	0.10 \pm 0.05	0.1 \pm 0.05
Lung	2.73 \pm 0.76	0.41 \pm 0.06	0.24 \pm 0.04	0.09 \pm 0.01	0.34 \pm 0.11	0.17 \pm 0.02
Liver	1.15 \pm 0.08	0.52 \pm 0.05	0.60 \pm 0.19	0.16 \pm 0.02	0.52 \pm 0.07	0.35 \pm 0.05
Spleen	0.99 \pm 0.10	0.18 \pm 0.08	0.20 \pm 0.18	0.05 \pm 0.03	0.13 \pm 0.09	0.09 \pm 0.06
Stomach	2.23 \pm 0.52	1.02 \pm 0.31	0.52 \pm 0.24	0.06 \pm 0.03	0.49 \pm 0.22	0.63 \pm 0.44
Kidneys	11.21 \pm 1.68	7.52 \pm 0.96	5.29 \pm 1.84	1.28 \pm 0.28	7.67 \pm 1.99	4.37 \pm 0.36*
Muscle	0.27 \pm 0.05	0.04 \pm 0.02	0.04 \pm 0.02	0.03 \pm 0.01	0.03 \pm 0.02	0.06 \pm 0.05
Pancreas	0.50 \pm 0.21	0.04 \pm 0.04	0.07 \pm 0.03	0.03 \pm 0.02	0.05 \pm 0.04	0.13 \pm 0.04
Bone	0.76 \pm 0.10	0.12 \pm 0.05	0.09 \pm 0.01	0.09 \pm 0.03	0.09 \pm 0.10	0.13 \pm 0.08
Skin	2.94 \pm 0.14	0.33 \pm 0.10	0.33 \pm 0.12	0.13 \pm 0.02	0.34 \pm 0.13	0.23 \pm 0.03
	Percent injected dose (%ID)					
Intestines	1.41 \pm 0.14	1.09 \pm 0.06	1.88 \pm 1.06	0.24 \pm 0.17	0.73 \pm 0.21	0.51 \pm 0.15
Urine	73.09 \pm 2.72	91.26 \pm 1.96	92.29 \pm 1.73	97.93 \pm 0.28	94.90 \pm 1.39	94.96 \pm 1.54
	Uptake ratio of tumor/normal tissue					
Tumor/liver	11.96	27.19	22.05	28.38	0.87	40.29
Tumor/kidney	1.23	1.88	2.50	3.55	0.06	3.23
Tumor/lung	5.03	34.49	55.13	50.44	1.32	82.94
Tumor/muscle	50.93	353.50	330.75	151.33	15.0	235.0
Tumor/blood	5.26	83.18	110.25	151.33	1.88	156.67
Tumor/skin	4.67	42.85	40.09	34.92	1.32	61.30

[#]2 h Data were cited from Table 2 for comparison;

* $p < 0.05$ for determining the significance of differences in tumor and kidney uptake between $^{99m}\text{Tc}(\text{EDDA})\text{-HYNIC-GGNle-CycMSH}_{\text{hex}}$ with or without NDP-MSH peptide blockade, as well as with or without L-lysine co-injection at 2 h post-injection.